

43. J. D. Vervoort, P. J. Patchett, *Geochim. Cosmochim. Acta* **60**, 3717 (1996).
44. V. J. M. Salters, W. M. White, *Chem. Geol.* **145**, 447 (1998).
45. J. D. Vervoort, P. J. Patchett, J. Blichert-Toft, F. Albarède, *Earth Planet. Sci. Lett.* **168**, 79 (1999).
46. J. Blichert-Toft, N. T. Arndt, *Earth Planet. Sci. Lett.* **171**, 439 (1999).
47. Supplemental U-Pb data are available at www.sciencemag.org/cgi/content/full/293/5530/683/DC1
48. A. H. Jaffey, K. F. Flynn, L. E. Glendenin, W. C. Bentley, A. M. Essling, *Phys. Rev. C* **4**, 1889 (1971).
49. K. R. Ludwig, *Geochim. Cosmochim. Acta* **62**, 665 (1998).
50. Deutsche Forschungsgemeinschaft funding (grant

ZG 3/16) is gratefully acknowledged. We thank R. Schott for the Hudson Highlands sample, K. Cameron for providing the UCSC Ames metal Lu-Hf solutions, and T. Kleine for productive discussions. Constructive reviews from two anonymous referees are greatly appreciated.

5 April 2001; accepted 15 June 2001

Very-Long-Period Seismic Signals and Caldera Formation at Miyake Island, Japan

Hiroyuki Kumagai,¹ Takao Ohminato,² Masaru Nakano,³ Masahiro Ooi,¹ Atsuki Kubo,¹ Hiroshi Inoue,¹ Jun Oikawa²

Over a period of roughly 40 days, starting on 8 July 2000, a caldera structure 1.7 kilometers in diameter developed by means of gradual depression and expansion of the summit crater at Miyake Island, Japan. At the same time, very-long-period (VLP) seismic signals were observed once or twice a day. Source mechanism analyses of the VLP signals show that the moment tensor solutions are smooth step functions over a time scale of 50 seconds, with dominant volumetric change components. We developed a model to explain the caldera and the VLP signals, in which a vertical piston of solid materials in the conduit is intermittently sucked into the magma chamber by lateral magma outflow. This model offers potential for making quantitative estimations of the characteristic physical properties of magma systems.

On Miyake Island (Fig. 1A), one of the Izu volcanic islands of Japan, quasiperiodic eruptions of basaltic magma have been recorded since 1085 A.D. (1). Three eruptions occurred in 1940, 1962, and 1983, with a rough-

ly 20-year interval and producing 10^7 m³ of erupted materials during each eruption (2). On 26 June 2000, an earthquake swarm beneath the island and anomalous changes of tiltmeters on the island indicated that magma intruded close to the surface along the southwestern flank (3). However, an eruption did not occur at that time and the earthquake swarm migrated toward Kozu Island, 40 km northwest of Miyake Island (Fig. 1A). On 8 July the first eruption occurred at the summit

crater of Miyake Island, and the depression of the summit crater began. The summit crater gradually sank and expanded until the middle of August, leaving a caldera 1.7 km in diameter (Fig. 1B) (4). At the same time, very-long-period (VLP) seismic signals were observed once or twice a day between 11 July and 18 August. During most of this period, there were only small eruptions, accompanied by ash ejections from the summit. The size of the summit eruptions increased gradually after 11 August, and the largest eruption that has occurred so far took place on 18 August. Sulfur dioxide (SO₂) gas emissions from the summit started on 29 August and have continued for more than 9 months. In contrast to the heightened SO₂ gas emissions, the earthquake swarm between Miyake and Kozu Islands gradually decreased after the largest eruption on 18 August.

The VLP signals showed similar impulsive waveforms (Fig. 2A), suggesting a repetitive and nondestructive source process. The VLP signals are not directly associated with eruptions but rather with a steplike inflation, followed by slow deflation recorded by the tiltmeters on the island (3). Source mechanism analyses of the VLP signals recorded by the Japanese broadband seismometer network (FREESIA/KIBAN) and a temporary seismic station on the island show that the source time functions of the moment tensor are represented by a smoothed step function over a

¹National Research Institute for Earth Science and Disaster Prevention, Tsukuba, Japan. ²Earthquake Research Institute, University of Tokyo, Tokyo, Japan. ³Graduate School of Environmental Studies, Nagoya University, Japan.

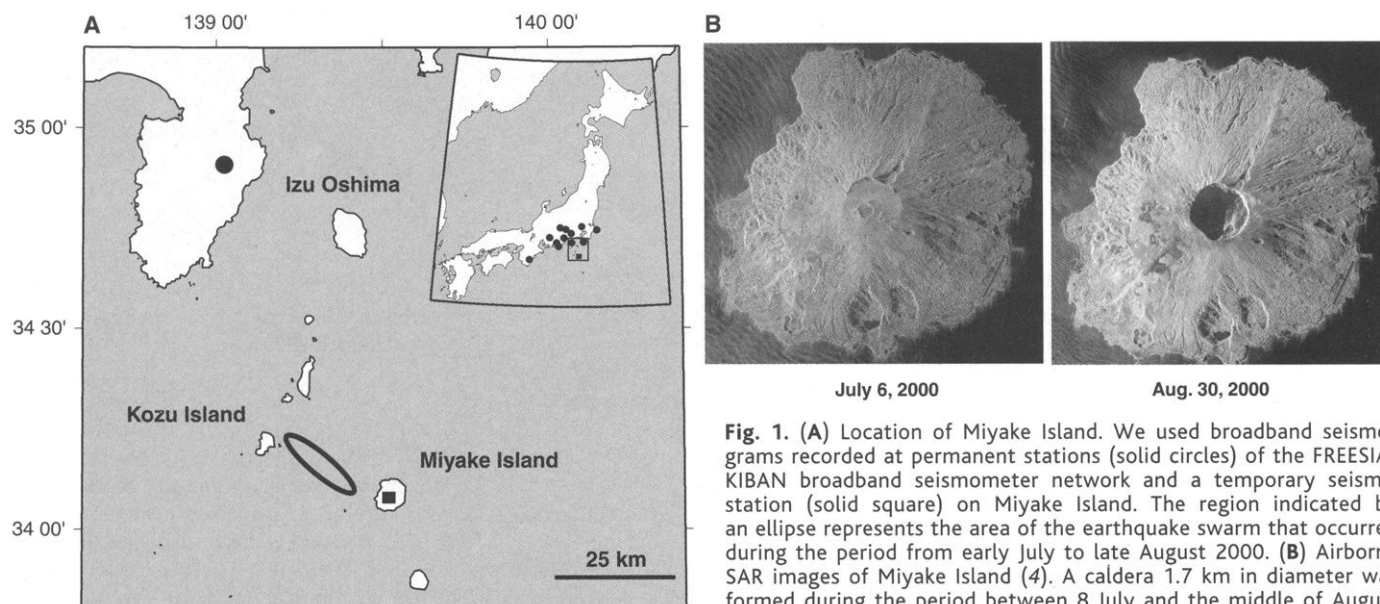


Fig. 1. (A) Location of Miyake Island. We used broadband seismograms recorded at permanent stations (solid circles) of the FREESIA/KIBAN broadband seismometer network and a temporary seismic station (solid square) on Miyake Island. The region indicated by an ellipse represents the area of the earthquake swarm that occurred during the period from early July to late August 2000. (B) Airborne SAR images of Miyake Island (4). A caldera 1.7 km in diameter was formed during the period between 8 July and the middle of August 2000 by gradual depression and expansion of the summit crater.

time scale of 50 s, with dominant volumetric change components (Fig. 2B) (5). This feature was obtained in all VLP signals, and the source duration was almost constant regardless of the size of the events. The estimated volumetric changes associated with the VLP signals (Fig. 3A) indicate that the events with larger volumetric changes tend to have longer occurrence time intervals. This suggests that the rate of the volumetric changes associated with the VLP signals is almost constant (Fig. 3B) and is about $4 \times 10^6 \text{ m}^3$ per day.

We propose a model that consists of a vertical piston representing solid materials in the conduit and magma chamber (Fig. 4) (6) to explain these observations. The load of the piston is balanced by friction at the wall between the piston and the surrounding medium and by the lithostatic and internal pressures in the magma chamber. As magma flows out of the chamber, the internal pressure in the chamber gradually decreases. The piston begins to move down into the chamber when the pressure decrease exceeds the static friction. As the piston intrudes into the chamber, the pressure in the chamber increases and the sliding velocity of the piston decreases. The chamber expands during the intrusion of the piston, generating the VLP signal. When the sliding velocity becomes zero, the upward acceleration of the piston is resisted by the recovered static friction, which stops the piston motion. The magma chamber slowly deflates because of the outflow of magma until the pressure decrease exceeds the static friction level. The above process then repeats itself.

The equation of motion for this model can be written as

$$m\ddot{z} = mg - F - p_1 S \quad (1)$$

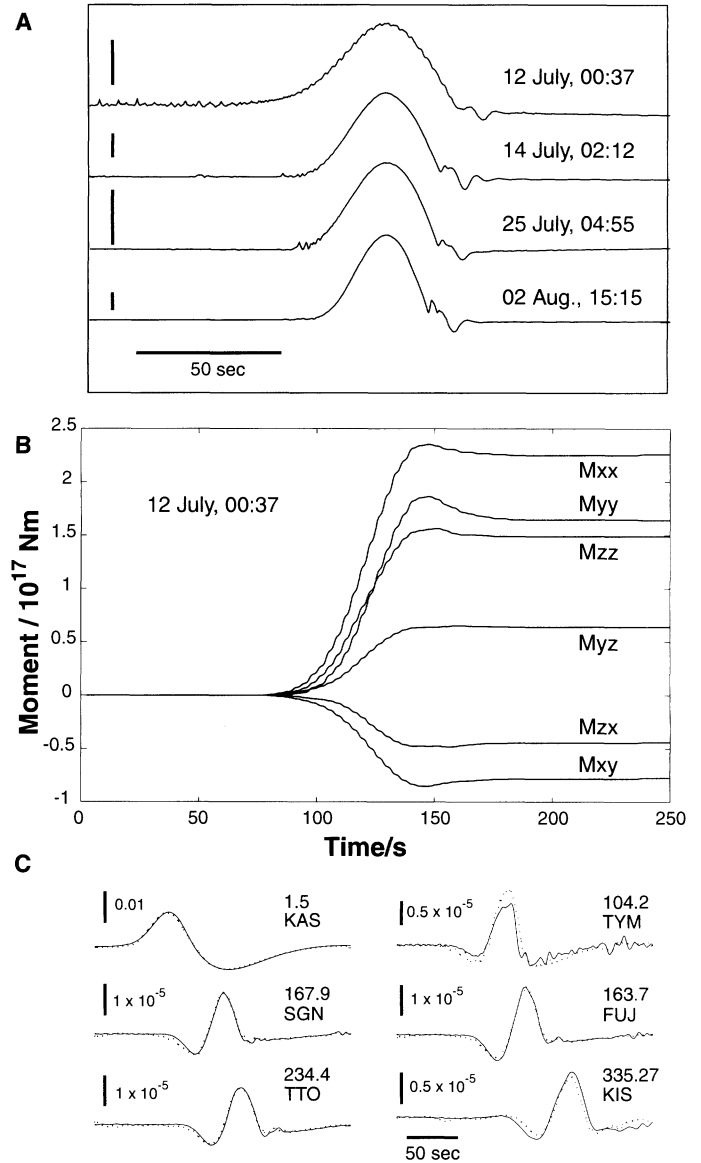
where z is the displacement of the piston, overdots denote time derivatives ($\ddot{z} = \partial^2 z / \partial t^2$) m is the mass of the piston, g is the gravitational acceleration, F is the total friction, p_1 is the pressure in the magma chamber, and S is the cross-sectional area at the base of the piston. We assume that p_1 is given by

$$p_1 = p_0 + \kappa \frac{(Sz - \alpha t)}{V_0} \\ = p_0 + p - p' t \quad (2)$$

where p_0 is an initial pressure, $p = \kappa Sz / V_0$ is the pressure increase due to the intrusion of the piston into the magma chamber, $p' = \kappa \alpha / V_0$ is the rate of pressure decrease due to the outflow of magma, V_0 is an initial volume of the magma chamber, κ is the bulk modulus of the magma, α is the outflow rate of the magma, and t is time. We assume that the friction F is characterized by static and dynamic frictions (7).

This equation of motion is similar to one for the block-spring model of stick-slip behavior on a fault (8). This equation can be

Fig. 2. (A) Vertical velocity waveforms of VLP signals observed at a temporary seismic station (KAS) on Miyake Island. These waveforms are corrected for instrumental response and are low-pass filtered with a corner frequency of 0.3 Hz. Vertical bars at the left of the seismograms indicate an amplitude of $5 \times 10^{-4} \text{ m/s}$. **(B)** The inversion result of the source time functions of six moment tensor components (M_{xx} , M_{yy} , M_{zz} , M_{xy} , M_{zx} , and M_{yz}) for the event that occurred on 12 July at 00:37 (Japan standard time), in which we use the band-passed displacement seismograms between 0.005 and 0.05 Hz (5). The Cartesian coordinates of x , y , and z correspond to N, E, and down. The amplitude ratios for the three principal axes of the moment tensor solution at 150 s are represented by 0.7:1:2.6, where the axis with the minimum amplitude ratio is slightly inclined (roughly 20°) from the vertical direction, and the axis with the maximum amplitude ratio points to the NW direction. This suggests the dilatation of a nearly vertical cracklike geometry at the source of the VLP signal. **(C)** Waveform match for the vertical components of the band-passed filtered displacement at six stations (KAS, SGN, TTO, TYM, FUJ, and KIS). The epicentral distances (in km) and amplitudes (in m) are indicated at the upper right and upper left corners of each seismogram, respectively. Solid and dotted lines represent observed and synthetic waveforms, respectively.



solved analytically, and the duration of the individual downward piston movement τ is given by

$$\tau = \frac{2\pi}{\omega} \left(1 - \frac{1}{\pi} \tan^{-1} \left\{ \frac{(F_s - F_d)\omega}{p'S} \right\} \right) \quad (3)$$

where $\omega = \sqrt{\kappa S^2 / V_0 m}$, and F_s and F_d are the static and dynamic frictions, respectively. The total displacement Δz of the individual downward piston movement is

$$\Delta z = \frac{p'S}{k} \tau + \frac{2(F_s - F_d)}{k} \quad (4)$$

where $k = \kappa S^2 / V_0$. The total volume change of the magma chamber due to the intrusion of the piston is then given by $S\Delta z$. The piston

begins to move after a time

$$T = \frac{2(F_s - F_d)}{p'S} \quad (5)$$

has elapsed. The piston moves down with a period of $\tau + T$. For $T \gg \tau$, Eq. 3 can be approximated as

$$\tau \sim \frac{\pi}{\omega} = \pi \sqrt{\frac{mV_0}{\kappa S^2}} \quad (6)$$

which depends only on the characteristic properties of the magma system.

Our source mechanism analyses show that $\tau \sim 50 \text{ s}$, $S\Delta z \sim 4 \times 10^6 \text{ m}^3$, and $T \sim 1 \text{ day}$. There exists a relation of $S\Delta z = \alpha T$ for $T \gg \tau$, and therefore we have $\alpha \sim 45 \text{ m}^3/\text{s}$. We

Fig. 3. (A) Estimated volume changes associated with the VLP signals plotted against time. We assume the Lamé's constants $\lambda = \mu = 20$ GPa to calculate the volume changes. (B) The cumulative plots of (A).

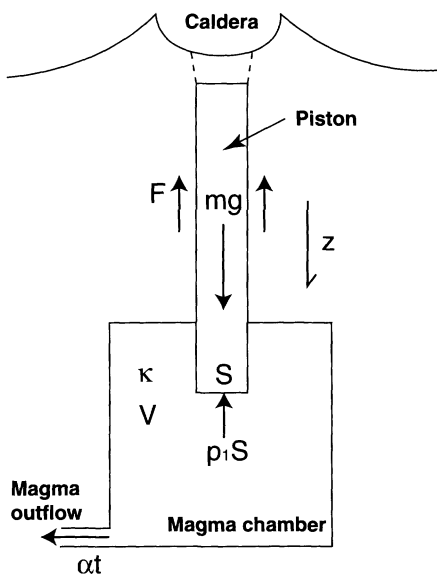
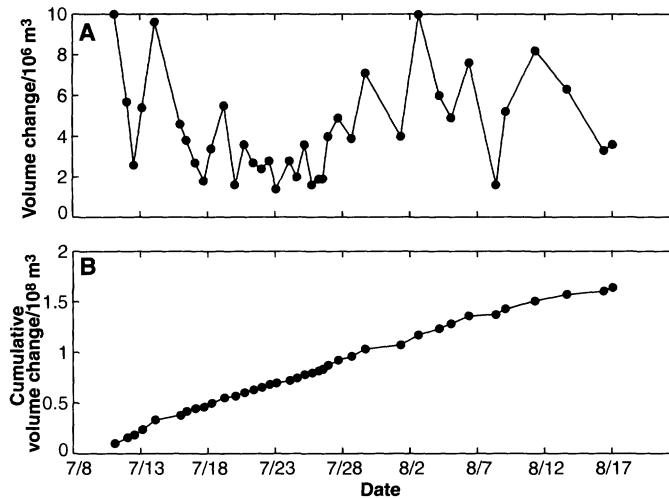


Fig. 4. A schematic diagram of a source process model of the VLP signals at Miyake Island, where z is the displacement of the piston, m is the mass of the piston, g is the gravitational acceleration, F is the friction, p_1 is the pressure in the magma chamber, S is the cross-sectional area at the base of the piston, V is the volume of the magma chamber, κ is the bulk modulus of the magma, α is the outflow rate of the magma, and t is time. The displacement z is positive downward.

adopt $\kappa = 1.8 \times 10^{10}$ Pa for basaltic magma and assume $S = 7.1 \times 10^4$ m² and $m = 6.2 \times 10^{11}$ kg for the piston (9), which result in $V_0 = 3.7 \times 10^{10}$ m³ and $F_s - F_d = 6.9 \times 10^{10}$ N. The calculated volume change of the magma chamber due to the intrusion of the piston ($z \times S$) for these parameter values shows a smoothed step function similar to the source time function estimated for the VLP signal (10). Furthermore, this model explains the following observations: (i) the almost constant source duration of the VLP signals regardless of event sizes, (ii) the signal with a larger volumetric change tending to have a longer occurrence interval, (iii) the steplike

inflation followed by slow deflation, and (iv) the synchronous occurrence of the caldera formation and the VLP signals. The second observation can be explained if $F_s - F_d$ varies in each event.

We estimate the volume of the magma chamber to be about 4×10^{10} m³. This value depends on the assumed piston properties and the bulk modulus of magma. The volume of the magma chamber decreases if we assume a narrower piston (9). The existence of bubbles in the magma may reduce the bulk modulus of the magma, resulting in a smaller magma chamber. It should be noted that the SO₂ gas emission from the summit requires a magma volume of about 7×10^6 m³ per day (11). The SO₂ gas emission has continued more than 9 months, resulting in a total magma volume of 1.9×10^9 m³ and more. Because the volume of the magma chamber should be greater than this value, our estimate of the volume of the magma chamber is consistent with this observation.

The basic process in our model is similar to one classified as the Kilauea-type collapse caldera (12). This type of caldera is found in basaltic volcanoes and may be formed by the depression caused by a magma flow out of the magma chamber. Although flank eruptions due to the magma flow were associated with caldera formation during the volcanic activity between 1959 and 1960 at Kilauea (13), no eruptions of large amounts of magma were associated with caldera formation at Miyake Island. However, the volcano-tectonic earthquake swarm between Miyake and Kozu Islands was observed during caldera formation and may have been caused by the magma flow out of the magma chamber. Our model helps to explain the formation of this type of caldera and may be applicable to other volcanoes, which may allow us to estimate characteristic properties of these magma systems.

References and Notes

1. N. Isshiki, *Bull. Volcanol.* **27**, 29 (1964).
2. T. Miyazaki, *Bull. Volcanol. Soc. Jpn.* **29**, S1 (1984); M. Tsukui, Y. Suzuki, *Bull. Volcanol. Soc. Jpn.* **43**, 149 (1998).

3. M. Ukawa *et al.*, *Earth Planets Space* **52**, xix (2000).
4. The Communications Research Laboratory took airborne synthetic aperture radar (SAR) images of Miyake Island using the x-band microwave. The airplane flew from north to south with a radio illumination direction from west to east for the images in Fig. 1B.
5. The source time functions of six moment tensor components were determined simultaneously by the inversion method of T. Ohminato *et al.* [*J. Geophys. Res.* **103**, 23839 (1998)]. The band-passed displacement seismograms between 0.005 and 0.05 Hz from 13 stations (Fig. 1A) were used in the inversions, assuming a point source. We used a horizontally layered structural model derived from refraction and reflection studies by A. Nishizawa *et al.* [*Programs Abstr. Seismol. Soc. Japan* **2**, A79 (1990)] to calculate Green's functions. Although single force components may be candidates for representing the source mechanism of the VLP signals, these components are strongly affected by source mislocations and uncertainty in the velocity model, which may cause fictitious results. Such an effect may be especially serious in our inversions because of a poor azimuthal coverage of the observations (Fig. 1A). We therefore restrict our inversions to the moment tensor components only in this study. Further inversions including single force components should be performed by using seismic as well as geodetic data on the island. In the moment tensor inversions, we conducted a grid search to find the best-fit point source location, which was determined at around 2 km south of the summit crater at a depth of around 5 km below sea level. Although the overall amplitudes of the moment tensor solutions increase with the increasing depth, the relative amplitudes of six moment tensor components in the solutions are less affected by changes in the source location, in which the increase of the source depth by 1 km causes about a 10% increase of the amplitudes, and the effect of horizontal changes in the source location is less than that of vertical changes. Our moment tensor solutions are consistent with those obtained independently by M. Kikuchi *et al.* [*J. Geogr.* **110**, 145 (2001)].
6. Models with a piston and a magma chamber have been conceptually proposed by K. Kazahaya *et al.* [*Eos* **81**, F1259 (2000)], M. Churei *et al.* [*Programs Abstr. Volcanol. Soc. Jpn.* **2**, 14 (2000)], and Y. Hayakawa [*Programs Abstr. Volcanol. Soc. Jpn.* **2**, 20 (2000)] based on geological, geochemical, and geodetic data.
7. We define the friction F as follows:

$$F = \begin{cases} (-\infty, F_s], & \dot{z} = 0 \\ F_d, & |\dot{z}| > 0 \end{cases}$$

where \dot{z} is the sliding velocity of the piston.

8. For examples, see D. L. Turcotte, G. Schubert, *Geodynamics* (Wiley, New York, 1982).
9. A cylindrical piston 300 m in diameter and 3500 m in length is assumed. The estimate of the piston length is based on hypocenter distributions of earthquakes beneath Miyake Island by S. Sakai *et al.* [*Programs Abstr. Seismol. Soc. Jpn.* **1**, A01 (2000)]. The hypocenter distributions suggest a vertically elongated structure located roughly beneath the center of the island down to 3 km below sea level, below which aseismic regions exist. We have no reliable estimate of the diameter of the conduit, which may range between 100 and 500 m. This range in conduit diameter means that the estimated volume of the magma chamber ranges from 4×10^9 m³ to 1×10^{11} m³.
10. Web fig. 1 is available on Science Online at www.sciencemag.org/cgi/content/full/293/5530/687/DC1.
11. The Geological Survey of Japan, Japan Meteorological Agency, and Tokyo Institute of Technology have continuously monitored the amount of SO₂ gas emissions using a correlational spectrometer (COSPEC) mounted on a helicopter. The average rate of SO₂ gas emission has been 4×10^4 metric tons per day since early September 2000. Assuming SO₂/H₂S ~ 3 and the sulfur content in magma to be 0.15 weight %, with a magma density of 2700 kg/m³, the volume of magma needed to provide the observed amount of SO₂ gas in one day is 7×10^6 m³. The sulfur content is adopted from one measured by K. Kazahaya *et al.* [*Eos* **81**, F1259 (2000)].

12. H. Williams, *Bull. Dep. Geol. Sci. Univ. Calif. Publ.* **25**, 239 (1941).
13. Summit eruption of Kilauea Iki crater in Hawaii began on 14 November 1959 and continued for more than 1 month, during which a volume of more than 3×10^7 m³ of lava erupted. After this summit eruption, eruption again occurred at Kapoha, some 40 km down the east rift zone from the Kilauea summit, on 13 January 1960 and continued until 19 February 1960, erupting more than

1.2×10^8 m³ of lava. During this eruption, the collapse of the Halemaumau floor, located 4 km west of Kilauea Iki crater, occurred. The collapse began on 6 February and stopped on 11 March. The total volume of collapse of Halemaumau was about 2×10^7 m³ [see J. P. Eaton, K. J. Murata, *Science* **132**, 925 (1960) and J. P. Eaton *et al.*, *U.S. Geol. Surv. Prof. Pap.* **1350**, 1307 (1987)].

14. We thank Y. Morita and members of the Earthquake Research Institute, University of Tokyo, for

acquiring waveform data at Miyake Island, and H. Watanabe for discussions. Comments from two anonymous reviewers helped improve the manuscript. Supported by the FREESIA project of the National Research Institute for Earth Science and Disaster Prevention and by the Japanese Ministry of Education under grant 12800011.

30 April 2001; accepted 5 June 2001

Egalitarianism in Female African Lions

Craig Packer,^{1*} Anne E. Pusey,¹ Lynn E. Eberly²

Because most cooperative societies are despotic, it has been difficult to test models of egalitarianism. Female African lions demonstrate a unique form of plural breeding in which companions consistently produce similar numbers of surviving offspring. Consistent with theoretical predictions from models of reproductive skew, female lions are unable to control each other's reproduction because of high costs of fighting and low access to each other's newborn cubs. A female also lacks incentives to reduce her companions' reproduction, because her own survival and reproduction depend on group territoriality and synchronous breeding. Consequently, female relationships are highly symmetrical, and female lions are "free agents" who only contribute to communal care when they have cubs of their own.

Animal societies are often characterized by disparities in female reproduction. Eusociality is defined by a system of queens and workers; many birds form groups with a single reproductive female and numerous "helpers at the nest" (1, 2). Carnivore species such as canids, mongooses, and meerkats show essentially the same pattern of a dominant reproductive female attended by subordinate helpers (3–6). Spotted hyenas form clans with multiple breeding females, but the top-ranking female garners greater reproduction than do subordinates (7), a pattern found to a varying extent across nonhuman primates (8–10). Theoretical models have highlighted circumstances in which female-female competition can lead either to despotism or egalitarianism, but most recent empirical research has focused on species showing extreme forms of skew. However, where related taxa show an almost universal trend toward despotism (11), a truly egalitarian species merits close examination—especially since egalitarianism may have promoted several of the emergent properties that characterize human society (12, 13).

Theoretical models predict that reproduction is most likely to be skewed where group productivity permits subordinates to tolerate a disproportionately small share of

reproduction, costly dispersal reduces the opportunity to escape manipulation by dominant companions, and kinship compensates helpers through inclusive fitness effects (14–18). Long-term studies suggest that African lions should be strongly predisposed toward reproductive skew: Pride-living females gain higher per capita reproduction than do solitaries or pairs, dispersing subadult females suffer reduced fitness, and female pridemates are always close genetic relatives (19–21). Yet lion prides are well known for containing multiple breeding females (22, 23).

Lions of the Serengeti National Park and Ngorongoro Crater, Tanzania, have been studied continuously since the 1960s (22, 24), and this analysis includes all births between 1963 and 1999. Reproduction can take place in any month of the year; gestation is 110 days, and the interbirth interval is about 2 years (25). Because of the secretive nature of females around parturition, we are unable to monitor all births, but we can track every cub that reaches its first birthday. Most juvenile mortality occurs in the first year of life (19); thus, we use the number of yearlings as our measure of lifetime reproductive success. Maternity is known for 80% of cubs but has to be attributed to candidate females in the remaining cases [also see (21)]. For example, if maternity cannot be assigned for three cubs reared by two mothers in a pride of seven females, we award 1.5 cubs to each mother and 0 cubs to the other five.

To quantify the degree of reproductive skew

in each pride, we compared the observed variance in lifetime reproduction across females to a distribution of 1000 simulated variances generated by the same reproductive rate and demography as the real pride but with births randomly allocated to each female (26). The first set of simulations only includes cubs of known maternity and thus overestimates the degree of skew by excluding a proportion of cases in which multiple females had in fact reared their cubs simultaneously. The second set uses all data, including cases of "shared maternity," and thus underestimates skew by apportioning shared cubs equally between candidate females. Testing the null hypothesis of random reproduction corresponds to testing whether the observed variance was more or less extreme than the simulated variances (P value = the proportion of simulated variances that were larger than the observed variance). Figure 1A illustrates the lifetime reproduction of individual females in a subset of eight prides: The three prides showing the lowest variances (and hence the highest degree of "evenness"), two representative prides showing intermediate evenness/skew, and the three prides showing the highest levels of skew.

The distribution of P values across all study prides is summarized in Fig. 1B. Overall, the within-pride variance in individual reproduction appears to be no greater than expected by chance. Restricting the data to cases of known maternity, only 1 of 24 prides (4.2%) showed a degree of skew that was significant ($P < 0.05$). Including all cases of inferred maternity, 3 of 31 prides (9.6%) showed higher evenness in individual reproduction than expected ($P > 0.95$). If lions showed a persistent tendency for even a partial degree of skew, there should have been an excess number of prides with P values in the 0.05 to 0.50 range, but there were about as many as would be expected if reproduction were random. The greatest case of skew occurred in a pride [TO (Fig. 1A)] where a lone female survived the death of her companions and spent most of her life as an unsuccessful solitary; the other two cases (MK and TI) resulted from the deaths of childless young females during disease outbreaks. Thus, demographic stochasticity contributes more to within-pride variation in individual reproduction than do any underlying differences in female reproductive performance.

Such egalitarianism is most likely to develop in species where one female is unable to

¹Department of Ecology, Evolution and Behavior, University of Minnesota, St. Paul, MN 55108, USA. ²Division of Biostatistics, School of Public Health, University of Minnesota, Minneapolis, MN 55455, USA.

*To whom correspondence should be addressed. E-mail: packer@biosci.umn.edu